

# Feature Selection with Annealing for Regression, Classification and Ranking

Adrian Barbu, Yiyuan She, Liangjing Ding, Gary Gramajo



arXiv:1310.2880v2 [stat.ML] 4 Jun 2014

**Abstract**—Many computer vision and medical imaging problems are faced with learning from large datasets, with millions of observations and features. In this paper we propose a novel efficient algorithm for variable selection and learning on such datasets, optimizing a likelihood with sparsity constraints. The iterative algorithm alternates parameter updates with tightening the constraints by gradually removing variables based on a criterion and a schedule. We present a generic approach for optimizing any differentiable loss function and present applications to regression, classification and ranking. We use one dimensional piecewise linear response functions to introduce nonlinear dependence on the selected variables and a second order prior on the response functions to avoid overfitting. We obtain theoretical guarantees of convergence and variable selection consistency for regression and logistic regression. Experiments on real and synthetic data show that the proposed method compares very well with other state of the art methods in regression, classification and ranking while being computationally very efficient.

**Index Terms**—feature selection, supervised learning, regression, classification, ranking.

## 1 INTRODUCTION

Many computer vision and medical imaging problems require learning classifiers from large amounts of data, with millions of observations and features. In these cases variable selection is important for speed and to obtain compact models that generalize well.

Boosting algorithms are used in many cases as they can handle large amounts of training data and can select a small number of features, based on the number of boosting iterations. However, each boosting iteration could be computationally expensive, especially since hundreds or even thousands of such iterations are usually required.

It is known [19] that boosting algorithms optimize a loss function (the exponential loss for Adaboost and logistic loss for Logitboost) by adaptive Newton steps at each boosting iteration. We are interested in finding out how the boosting algorithms compare with algorithms that directly optimize the same loss function by gradually removing variables. The proposed approach is different from those existent in the literature since at each

iteration, instead of adding a variable that decreases the loss most (as Boosting algorithms do), at each iteration a number of variables are removed while the model parameters are updated.

At each iteration, the optimization algorithm performs one gradient update step of the model parameters and a selection step that removes variables based on the coefficient magnitudes. More than one variable is usually removed at a time, according to a predefined schedule.

The proposed method can handle large datasets without being online. The total amount of data the algorithm needs for training is equivalent to about 2-10 passes through the whole training set, which can be orders of magnitude faster than Boosting. The algorithm can be distributed on a grid of processors for large scale problems.

Experiments on real and synthetic data show that the proposed method usually outperforms Logitboost and penalized methods and at the same time it is faster.

## 2 THE FEATURE SELECTION WITH ANNEALING ALGORITHM

Let  $(\mathbf{x}_i, y_i), i = \overline{1, N}$  be training examples with  $\mathbf{x}_i \in \mathbb{R}^M$  and a loss function  $L(\beta)$  defined based on these examples. We are interested in the constrained optimization of the loss function

$$\beta = \underset{\{j: \beta_j \neq 0\} \leq k}{\operatorname{argmin}} L(\beta) \quad (1)$$

where the number  $k$  of relevant features is a given parameter. Further assume that the loss function  $L(\beta)$  is differentiable with respect to  $\beta$ .

### 2.1 Algorithm Description

The proposed approach starts with an initial value of the parameters  $\beta$ , usually  $\beta = 0$ , and alternates two basic steps:

- one step of parameter updates towards minimizing the loss  $L(\beta)$  by gradient descent

$$\beta \leftarrow \beta - \eta \frac{\partial L(\beta)}{\partial \beta} \quad (2)$$

- one variable selection step that removes some variables according to the coefficient magnitudes  $|\beta_j|, j = \overline{1, M}$ .

---

• A. Barbu, Y. She and G. Gramajo are with the Department of Statistics, Florida State University, Tallahassee, Florida 32306, USA, Fax: 850-644-5271, Email: abarbu@stat.fsu.edu, yshe@stat.fsu.edu, ggramajo@stat.fsu.edu.

Usually many variables are removed in each of the first few iteration, keeping only a number  $M_e$  of variables that have the largest values of  $|\beta_j|$ . The number  $M_e$  of variables that are kept after each iteration  $e = \overline{1, N^{iter}}$  is similar to an annealing schedule.

Through this schedule, the constraint after iteration  $e$  is  $|\{j, \beta_j \neq 0\}| \leq M_e$ , thus the constraint is gradually tightened and after a large number of iterations we reach  $|\{j, \beta_j \neq 0\}| \leq k$ . This way we obtain a locally optimal solution to the constrained problem (1).

In this work we will use an inverse schedule  $M_e, e = \overline{1, N^{iter}}$  with a parameter  $v$  or  $\mu = \frac{M}{kv}$

$$M_i = \max(k, \frac{M}{1 + i\mu} - \frac{1}{N^{iter}}). \quad (3)$$

Because the  $M_e$  quickly decreases after the first iteration, the total computation time of the algorithm is about  $N(M + kv \ln \frac{M}{k} + kN^{iter})$  operations, where  $N$  is the number of training examples, assuming one iteration with  $M$  variables takes  $MN$  operations. Thus when  $N^{iter} = 500$ , and  $k$  is not too large, the whole algorithm takes about  $2MN$  operations.

In Figure 1 are shown the value of  $M_e$  vs the iteration number  $e$  for three schedules  $v = 50, 100$  and  $200$ , where  $M = 10,000$  and  $k = 10$ . We also experimented with an exponential schedule  $M_e = \max(k, M\xi^e)$  with a parameter  $0 < \xi < 1$ , but observed that the inverse schedule worked better for the same computational expense.

The proposed algorithm is summarized in Algorithm 1.

---

#### Algorithm 1 Feature Selection with Annealing (FSA)

---

**Input:** Training examples  $\{(x_i, y_i)\}_{i=1}^N$ .

**Output:** Trained classifier parameter vector  $\beta$ .

- 1: Initialize  $\beta = 0$ .
  - 2: **for**  $e=1$  to  $N^{iter}$  **do**
  - 3: Update  $\beta \leftarrow \beta - \eta \frac{\partial L(\beta)}{\partial \beta}$
  - 4: Keep the  $M_e$  variables with highest  $|\beta_j|$  and renumber them  $1, \dots, M_e$ .
  - 5: Set  $M = M_e$
  - 6: **end for**
- 

The prototype FSA algorithm is extremely simple to implement. In Section 2.2, we provide exact choices of  $\eta$  for the gradient step theoretically. Step 4 conducts an adaptive keep-or-kill selection, which results in a nonlinear operator and increases the difficulty of the theoretical analysis. It is worth pointing out that the selection criterion is not ad-hoc like in most back elimination approaches and does not involve any information of the loss; however, this simple norm-based design has a rigorous guarantee of convergence and consistency.

The performance of the FSA algorithm depends on the following parameters:

- Gradient learning rate  $\eta$ , which can be arbitrarily small provided that the number of iterations is large enough. If  $\eta$  is too large, the coefficients  $\beta_j$  will not

converge. In all our experiments we used  $\eta = 20$  for classification and  $\eta = 1$  for regression.

- Parameter  $v$  or  $\mu$  for controlling the number of variables left at each iteration. Parameter  $\mu$  should have a value proportional to the learning rate  $\eta$  so that if the learning rate is small, the variables are removed at a slower pace.
- Number of iterations  $N^{iter}$ , large enough to obtain in the end a desired number  $k$  of variables and to insure the parameters have converged to a desired tolerance. In our experiments we used  $N^{iter} = 500$ .

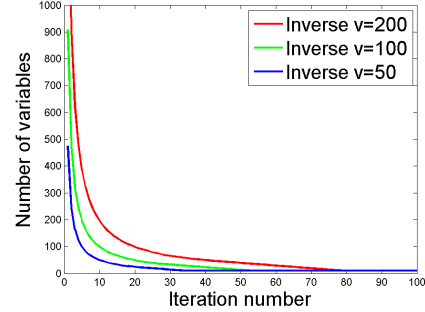


Fig. 1. The value of the number of selected features  $M_e$  vs iteration  $e$  for three annealing schedules, where  $M = 10,000, k = 10$ .

We will present in Section 3.1 an evaluation of the stability of the algorithm with respect to these parameters for a classification problem. We will see that the performance of the algorithm is stable for a large range of values for the parameters  $\eta, \mu, N^{iter}$ .

The FSA algorithm can be used for the optimization of any differentiable loss function subject with a sparsity constraint as described in eq. (1). In this paper we will look at three standard loss functions, the quadratic loss in regression, the logistic loss in classification and the differential loss from [8] for ranking.

#### 2.1.1 FSA for Regression

Given training examples  $(x_i, y_i) \in \mathbb{R}^M \times \mathbb{R}, i = \overline{1, N}$ , we have the penalized squared-error loss

$$L(\beta) = \sum_{i=1}^N (y_i - x_i^T \beta)^2 + \sum_{j=1}^M \rho(\beta_j) \quad (4)$$

with a differentiable prior function  $\rho$ . This loss has the partial derivatives

$$\frac{\partial L(\beta)}{\partial \beta_j} = \sum_{i=1}^N (x_i^T \beta - y_i) x_{ij} + \rho'(\beta_j), j = \overline{1, M}$$

#### 2.1.2 FSA for Classification, Logistic Loss

Given training examples  $(x_i, y_i) \in \mathbb{R}^M \times \{0, 1\}, i = \overline{1, N}$ , we have the penalized logistic loss

$$L(\beta) = -\sum_{i=1}^N w_i \ln(1 + \exp(-\tilde{y}_i x_i^T \beta)) + \sum_{j=1}^M \rho(\beta_j) \quad (5)$$

where  $\tilde{y}_i = 2y_i - 1 \in \{-1, 1\}$ . This loss has the partial derivatives

$$\begin{aligned}\frac{\partial L(\boldsymbol{\beta})}{\partial \beta_j} &= \sum_{i=1}^N w_i \tilde{y}_i x_{ij} \frac{\exp(-\tilde{y}_i \mathbf{x}_i^T \boldsymbol{\beta})}{1 + \exp(-\tilde{y}_i \mathbf{x}_i^T \boldsymbol{\beta})} + \rho'(\beta_j) \\ &= \sum_{i=1}^N w_i x_{ij} (y_i - p(\mathbf{x}_i)) + \rho'(\beta_j)\end{aligned}$$

where

$$p(\mathbf{x}) = \tilde{p}(y = 1|\mathbf{x}) = \frac{1}{1 + \exp(-\mathbf{x}^T \boldsymbol{\beta})} \quad (6)$$

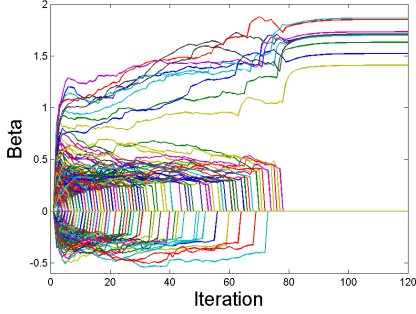


Fig. 2. The value of  $\beta_j, j = \overline{1, M}$  vs iteration number for simulated data with  $N = 1000, M = 1000, k = 10$  with  $\eta = 20, v = 200$ .

In Figure 2, are shown the  $\beta_j, j = \overline{1, M}$  vs iteration number for a linear classification problem with  $N = 1000$  observations and  $M = 1000$  variables described in Section 3.2. After each iteration, some of the  $\beta_j$  are made zero according to the schedule  $M_e$ .

The FSA for regression and logistic regression enjoy consistency guarantees that are presented in the next section and proved in the supplementary material.

### 2.1.3 FSA for the SVM Loss

Given training examples  $D = \{(\mathbf{x}_i, y_i) \in \mathbb{R}^M \times \{-1, 1\}, i = \overline{1, N}\}$ , the FSA for SVM optimizes the differentiable approximation of the primal SVM objective function from [9]

$$L_D(\boldsymbol{\beta}) = \sum_{i=1}^N L_h(y_i f_{\boldsymbol{\beta}}(\mathbf{x}_i)) + \sum_{j=1}^M \rho(\beta_j) \quad (7)$$

where  $L_h : \mathbb{R} \rightarrow \mathbb{R}$  is the Huber-style differentiable approximation of the hinge loss [9]:

$$L_h(x) = \begin{cases} 0 & \text{if } x > 1 + h \\ \frac{(1 + h - x)^2}{4h} & \text{if } |1 - x| \leq h \\ 1 - x & \text{if } x < 1 - h \end{cases} \quad (8)$$

## 2.2 Convergence and Consistency Theorem

We investigate the performance of the FSA estimators theoretically in both *regression* and *classification* problems. In the first case,  $y_i$  has a Gaussian distribution  $\mathcal{N}(\mathbf{x}_i^T \boldsymbol{\beta}^*, \sigma^2 I)$ , while in the latter situation  $y_i$  are binary following the Bernoulli distribution with mean  $\mathbf{x}_i^T \boldsymbol{\beta}^*$ . The log-likelihood based loss (denoted by  $F$ ) is the squared-error loss and the logistic loss from eq. (5) and

(4) respectively. For clarity, we redefine them as follows:

$$\textbf{Regression: } F(\boldsymbol{\beta}) = \frac{1}{2} \sum_{i=1}^N (y_i - \mathbf{x}_i^T \boldsymbol{\beta})^2, \quad (9)$$

$$\textbf{Classification: } F(\boldsymbol{\beta}) = \sum_{i=1}^N (-y_i \mathbf{x}_i^T \boldsymbol{\beta} + \log(1 + \exp(\mathbf{x}_i^T \boldsymbol{\beta}))). \quad (10)$$

Although  $M$  is large (possibly much greater than  $N$ ), the problem is still well-posed because the true coefficient vector  $\boldsymbol{\beta}^*$  is assumed to be sparse in the sense that  $\|\boldsymbol{\beta}^*\|_0 \leq k < N$ , where  $\|\boldsymbol{\beta}\|_0 := |\{j : \beta_j \neq 0\}|$ .

Let  $\{\boldsymbol{\beta}^{(e)}\}$  be the value of  $\boldsymbol{\beta}$  at iteration  $e$  in the algorithm. Let  $M_e$  be a bounded and monotone annealing schedule satisfying  $M \geq M_e \geq k, \forall e$  and  $M_e = k$  for sufficiently large values of  $e$ . Suppose  $L = F$  (for now) in either regression or classification.

*Theorem 2.1:* The following convergence and consistency results hold under  $0 < \eta < 4/\|\mathbf{X}\|_2^2$  for classification and  $0 < \eta < 1/\|\mathbf{X}\|_2^2$  for regression, respectively, where  $\|\mathbf{X}\|_2$  stands for the spectral norm of the design:

(i) The algorithm converges (assuming  $N^{iter} = +\infty$ ) in the sense that  $F(\boldsymbol{\beta}^{(e)})$ , for sufficiently large values of  $e$ , decreases monotonically to a limit.

(ii) In regression (cf. (9)),  $\lim_{e \rightarrow \infty} \boldsymbol{\beta}^{(e)}$  always exists; in classification (cf. (10)), under the overlap condition in the appendix, the same conclusion holds. Moreover, the limit point is a locally optimal solution to  $\min_{\boldsymbol{\beta}: \|\boldsymbol{\beta}\|_0 \leq k} F(\boldsymbol{\beta})$ .

(iii) Suppose, asymptotically,  $N \rightarrow +\infty$  and the limit of the scaled Fisher information matrix exists, i.e., the design  $\mathbf{X}(N)$  and true coefficient  $\boldsymbol{\beta}^*$  satisfy  $\lim \mathbf{X}^T \mathbf{X}/N \rightarrow \mathcal{I}^*$  in regression, or  $\lim \mathbf{X}^T \text{diag} \left\{ \frac{e^{\mathbf{x}_i^T \boldsymbol{\beta}^*}}{(1 + e^{\mathbf{x}_i^T \boldsymbol{\beta}^*})^2} \right\} \mathbf{X}/N \rightarrow \mathcal{I}^*$  in classification, for some  $\mathcal{I}^*$  positive definite. Then, there exists a slow enough schedule  $\{M_e\}$  such that *any*  $\boldsymbol{\beta}^{(e)}$  for  $e$  sufficiently large is a consistent estimator of  $\boldsymbol{\beta}^*$ , and  $\{j : \beta_j^* \neq 0\} \subset \{j : \beta_j^{(e)} \neq 0\}$  occurs with probability tending to 1.

*Remark.* The theorem holds more generally, for many smoothly penalized loss criteria. For example, when  $L = F + \frac{1}{2} \lambda \|\boldsymbol{\beta}\|_2^2$ , (i) and (ii) are true for any  $\lambda > 0$ , with no need of the overlap assumption in classification (the proof is similar yet simpler). Due to space limitations, such results and proof details are not shown in this work.

## 2.3 Related Work

Boosting algorithms – such as Adaboost [35], Logitboost [19], Floatboost [31], Robust Logitboost [30] to cite only a few – optimize a loss function in a greedy manner in  $k$  iterations, at each iteration adding a weak learner that decreases the loss most. Boosting algorithms can be used for feature selection by making the weak learners depend on a single variable (feature). What feature will be selected in the next boosting iteration depends on what features have already been selected and their coefficients. This dependence structure makes it difficult to obtain theoretical variable selection guarantees for boosting.

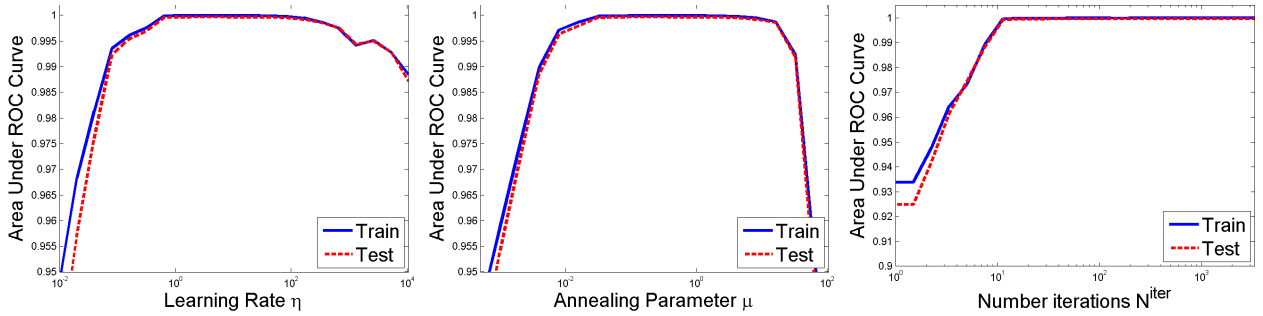


Fig. 3. Dependence of the AUC vs algorithm parameters for a linear dataset with  $M = N = 1000$ ,  $k = k^* = 10$ . Left: dependence on  $\eta$ . Middle: dependence on  $\mu$  when  $\eta = 20\mu$ . Right: dependence on  $N^{iter}$ .

The approach introduced in this paper is different from boosting because it starts with all the variables and gradually removes variables, according to an elimination schedule, so it is a backward elimination method [20], and we can offer theoretical guarantees of convergence, variable selection and parameter consistency.

Some works [33], [19] propose ways to introduce shrinkage in the boosting framework to control the generalization ability. Shrinkage and even higher order priors can be easily introduced in the approach we propose in this paper.

Penalized loss algorithms add a sparsity inducing penalty such as the  $L_1$ [6], [12], [24], [41], SCAD[16], MCP[40] and the  $L_0 + L_2$  [36], [37] and optimize the penalized loss in different ways. The proposed method is different from the penalized methods because variable selection is not obtained by imposing a sparsity prior on the variables, but by a direct optimization of the  $L_0$  constrained loss function.

By directly minimizing the constrained loss function, the proposed approach does not introduce any undesired bias on the coefficients. Any desired biases (e.g. shrinkage) can be introduced as priors in the loss function  $L(\beta)$ . In contrast, the bias introduced by the  $L_1$  penalty for a certain sparsity level might be too large and it can lead to poor classification performance [5], [13], [16].

In [15] a screening procedure analyzed each variable by fitting a model that depends only on that variable. In contrast, our screening procedure fits a model that depends on all variables and gradually removes them according to a schedule.

The closest related work is the Thresholding based Iterative Selection Procedure (TISP), HardTISP and QuantileTISP in particular [36], [37] which optimizes a penalized loss function by alternating coefficient updates and thresholding. However, it does not remove the variables according to a schedule.

The proposed method is inspired by TISP and by the Graduated Nonconvexity Algorithm [3] that optimizes a non-convex Markov Random Field by starting optimizing a convex surrogate and gradually changing the function to be optimized towards the desired non-convex formulation, initializing each optimization step with the result from the previous step.

The proposed method is quite similar to the Recursive

Feature Elimination [21] (RFE) procedure, which alternates training an SVM classifier on the current feature set and removing a percentage of the features based on the magnitude of the variable coefficients. However, our approach has the following differences:

- 1) It removes variables long before the parameters  $\beta$  have converged, thus it can be many orders of magnitude faster than the RFE approach where the coefficients are fully trained at each iteration.
- 2) It can be applied to any loss function, not necessarily the SVM loss and we present applications in regression, classification and ranking.
- 3) It offers theoretical guarantees of variable selection and parameter consistency.

### 3 SIMULATION EXPERIMENTS

We first present simulations on synthetic data to evaluate feature selection and prediction performance and compare it with other state of the art feature selection methods.

The data for simulations has correlated predictors sampled from a multivariate normal  $x \sim \mathcal{N}(0, \Sigma)$  where  $\Sigma_{ij} = \delta^{|i-j|}$  and  $\delta = 0.9$ .

For classification, label  $y$  for a data point  $x \in \mathbb{R}^M$  is

$$y = \begin{cases} 1 & \text{if } \sum_{i=1}^{k^*} x_{10i} > 0 \\ 0 & \text{otherwise} \end{cases} \quad (11)$$

Thus the data is linearly separable and only the variables with index  $10i$ ,  $i = 1, k$  are relevant.

All experiments were performed on a six core Intel Core I7-980 machine at 3.3GHz with 24Gb RAM.

#### 3.1 Stability with Respect to Parameters

In this experiment, we evaluate the stability of the FSA Algorithm 1 with respect to its tuning parameters: the learning rate  $\eta$ , the annealing rate  $\mu$  and the number of iterations  $N^{iter}$ . The experiment was conducted on the linearly separable data with  $M=N=1000$ ,  $k=k^*=10$ .

In Figure 3 are shown the dependence of the average area under the ROC curve (AUC) with respect to  $\eta$  (left),  $\mu$  (middle) and  $N^{iter}$  (right). For the left plot, we had  $\mu = 1$ ,  $N^{iter} = 500$ , for the middle plot  $\eta = 20\mu$ ,  $N^{iter} = 500$  and for the right plot  $\mu = 1$ ,  $\eta = 20$ . The obtained curves are the averages of 10 runs.

One can see that all three parameters have a large range of values that yield optimal prediction performance.

TABLE 1

Classification experiments on simulated linearly separable data with  $\delta = 0.9$ , averaged over 100 runs.

			Variable detection rate								Test AUC							
$N$	$M$	$k=k^*$	FSA	FSASVM	TSP	$L_1$	MCP	SCD	LB	LB1	FSA	FSASVM	TSP	$L_1$	MCP	SCD	LB	LB1
300	1000	10	<b>31</b>	30	0	0	3	1	0	0	<b>0.991</b>	0.990	0.889	0.891	0.956	0.934	0.950	0.920
300	10000	10	<b>21</b>	21	0	0	4	4	1	0	<b>0.986</b>	0.983	0.827	0.881	0.938	0.921	0.946	0.911
1000	1000	10	<b>100</b>	100	1	2	39	25	44	0	<b>1.000</b>	1.000	0.947	0.925	0.967	0.953	0.967	0.933
3000	1000	10	<b>100</b>	100	30	33	65	63	97	0	<b>1.000</b>	1.000	0.987	0.971	0.975	0.973	0.971	0.937
1000	1000	30	<b>23</b>	22	0	0	0	0	0	0	<b>0.997</b>	0.995	0.918	0.883	0.955	0.937	0.956	0.937
3000	1000	30	<b>100</b>	100	0	0	8	14	4	0	<b>1.000</b>	1.000	0.969	0.919	0.979	0.976	0.976	0.947

### 3.2 Classification Experiments

In this experiment we compare the variable selection and the prediction performance of the FSA algorithm with different regularized loss methods and with the Logitboost algorithm. Logitboost can be used for feature selection if each weak learner depends on only one variable.

The experiments are performed on the linearly separable data described above. The algorithms being compared are:

- 1) FSA - The FSA Algorithm 1 for the logistic loss (5) with the  $v = 200$  annealing schedule,  $\eta = 20$ .
- 2) FSASVM - The FSA Algorithm 1 for the SVM loss (7) with the  $v = 200$  annealing schedule,  $\eta = 1$ .
- 3) TSP - The quantile TISP algorithm with 10 thresholding iterations and 500 more iterations on the selected variables for convergence.
- 4)  $L_1$  - The interior point method [26] for  $L_1$ -penalized Logistic Regression using the implementation from [http://www.stanford.edu/~boyd/l1\\_logreg/](http://www.stanford.edu/~boyd/l1_logreg/). To obtain a given number  $k$  of variables, the value of the  $L_1$  penalty  $\lambda$  is found using the bisection method [7]. The bisection procedure calls the interior point training routine about 9 times until a  $\lambda$  is found that gives exactly  $k$  nonzero coefficients.
- 5) MCP - Logistic regression using MCP (Minimax Concave Penalty)[40]. Two implementations were evaluated: the `ncvreg` R package based on the coordinate descent algorithm [4] and the `cvplogistic` R package based on the Majorization-Minimization by Coordinate Descent (MMCD) algorithm [23]. The `cvplogistic` package obtained better results, which are reported in this paper.
- 6) SCD - The two R packages `ncvreg` and `cvplogistic` also implement the SCAD penalty, with the `cvplogistic` package obtaining better results, reported in this paper.
- 7) LB - Logitboost using univariate linear regressors as weak learners. In this version, all  $M$  linear regressors (one for each variable) are trained at each boosting iteration and the best one is added to the classifier.
- 8) LB1 - Similar to LB, but only 10% of the learners were selected at random and trained at each boosting iteration and the best one was added to the classifier.

In Table 1 are shown the variable detection rate and

the Area under the ROC curve (AUC) on unseen data of same size as the training data, obtained from 100 independent runs. The variable detection rate is the percentage of times when all  $k^*$  variables were correctly found i.e.  $\{j, \beta_j \neq 0\} = \{i, \beta_i^* \neq 0\}$ . The average training times for the methods being evaluated are shown in Table 2.

TABLE 2

Average training times (seconds) for the experiments from Table 1.

$N$	$M$	$k$	FSA	FSASVM	TSP	$L_1$	MCP	SCD	LB	LB1
300	1000	10	0.03	0.03	0.02	17	87	68	0.13	0.01
300	10000	10	0.09	0.09	0.12	1240	749	644	1.5	0.15
1000	1000	10	0.06	0.07	0.05	469	352	282	0.44	0.09
3000	1000	10	0.23	0.15	0.21	705	1122	1103	1.3	0.18
1000	1000	30	0.13	0.08	0.05	240	358	293	1.2	0.16
3000	1000	30	0.26	0.2	0.29	565	1840	1139	4.1	0.48

The FSA algorithm detects the true variables more often and obtain significantly better ( $p$ -value  $< 10^{-4}$ ) AUC numbers than the other algorithms. At the same time the training time is reduced by three orders of magnitude compared to the penalized methods and is on par with TISP and Logitboost. We also observe that given sufficient training data, the FSA algorithm will always find the true variables and learn a model that has almost perfect prediction on the test data. These findings are in accord with the theoretical guarantees of convergence and consistency from Theorem 2.1.

There exist algorithms [28], [39] for  $L_1$ -penalized logistic regression in the literature that are faster than [26]. Even though the training times might be greatly reduced, these algorithms optimize the same  $L_1$  penalized loss function as [26], so the variable detection rates and AUC's should be similar to or worse than those in Table 1.

### 3.3 Regression Experiments

Similar to the classification simulations, the observations are sampled from a multivariate normal  $\mathbf{x} \sim \mathcal{N}(0, \Sigma)$  where  $\Sigma_{ij} = \delta^{|i-j|}$  and  $\delta = 0.9$ . Given  $\mathbf{x}$ , the dependent variable  $y$  is obtained as

$$y = \sum_{i=1}^{k^*} x_{10i} + \epsilon, \quad \epsilon \sim \mathcal{N}(0, 1)$$

We experimented with different data sizes and number  $k^*$  of relevant variables. The results of the experiments, averaged over 100 runs, are given in Table 3.

The following algorithms were evaluated:

TABLE 3

Regression experiments on simulated data with correlation  $\delta = 0.9$ , averaged over 100 runs.

Data Params.			Var. det. rate					RMSE					Time(s)				
$N$	$M$	$k$	FSA	TSP	L1	MCP	SCAD	FSA	TSP	L1	MCP	SCAD	FSA	TSP	L1	MCP	SCAD
1000	100	3	100	4	100	100	85	1.01	1.37	1.00	1.00	6.98	0.05	0.01	0.07	0.11	0.05
300	1000	30	67	0	0	0	0	1.25	5.14	3.75	50.8	141.9	0.25	0.09	0.34	1.56	0.15
300	10000	30	4	0	0	0	0	2.29	5.90	3.74	333	437.4	0.22	0.12	2.76	18.6	3.55
1000	10000	30	100	0	0	13	0	1.03	4.53	2.99	193.1	437.4	0.58	0.25	4.03	66.2	14.9
1000	10000	100	79	0	0	0	0	1.17	9.61	6.64	370.4	440.6	0.74	0.46	6.85	361	48.5
3000	10000	100	100	0	0	0	0	1.04	7.97	5.44	370.3	440.6	2.60	1.90	15.4	239	98.6

- 1) FSA - The FSA Algorithm 1 with the  $v = 200$  annealing schedule,  $\eta = 20$ .
- 2) TSP - The quantile TISP algorithm with 10 thresholding iterations and 500 more iterations on the selected variables for convergence.
- 3)  $L_1$  - The built in `lasso` function from Matlab
- 4) MCP, SCD. The MCP and SCAD penalized regression using coordinate descent [4]. The `ncvreg C++` implementation was used.

One could see from Table 3 that the FSA algorithm consistently finds the true variables more often than the other methods and obtains better predictions in terms of root mean square error (RMSE) than the other methods. We also observe that the FSA algorithm scales very well to large data sizes, in fact it scales as  $O(MN)$  where  $N$  is the number of observations and  $M$  is the number of variables.

## 4 CAPTURING NONLINEARITY IN REGRESSION AND CLASSIFICATION

In this section we present methods based on the FSA technique to capture nonlinearity and structural information in the feature space for feature selection.

We will use a type of nonlinearity that is compatible with feature selection, obtained by replacing  $\beta x$  with a nonlinear response function that is a sum of a number of univariate functions

$$f_{\beta}(x) = \sum_{j=1}^M f_{\beta_j}(x_j), \quad (12)$$

where  $\beta_j$  is a parameter vector characterizing the response function on variable  $j$ .

The univariate functions we will use are piecewise linear, as described in the next section.

### 4.1 Piecewise Linear Learners

A piecewise linear (PL) learner  $f_{\beta}(x) : \mathbb{R} \rightarrow \mathbb{R}$  is a piecewise function that only depends on one variable  $x$  of the instance  $x \in \Omega$ . It is defined based on the range  $[x^{min}, x^{max}]$  of that variable and a predefined number  $B$  of bins.

Let  $b = (x^{max} - x^{min})/B$  be the bin length.

For each value  $x$ , the learner finds the bin index  $j(x) = \lceil (x - x^{min})/b \rceil \in \{0, \dots, B - 1\}$  and the relative position in the bin  $\alpha(x) = (x - x^{min})/b - j(x) \in [0, 1)$  and returns

$$f_{\beta}(x) = \beta_{j(x)}(1 - \alpha(x)) + \beta_{j(x)+1}\alpha(x)$$

Let

$$u_i(x) = \begin{cases} 1 - \alpha(x) & \text{if } i = j(x) \\ \alpha(x) & \text{if } i = j(x) + 1 \\ 0 & \text{else} \end{cases}$$

for  $i \in \{0, \dots, B\}$  be a set of  $B + 1$  piecewise linear basis functions. Then  $f_{\beta}(x)$  can be written as a linear combination:

$$f_{\beta}(x) = \sum_{i=0}^B \beta_i u_i(x) = \mathbf{u}^T(x) \boldsymbol{\beta}$$

where  $\mathbf{u}(x) = (u_0(x), \dots, u_B(x))^T$  is the vector of responses of the basis functions and  $\boldsymbol{\beta} = (\beta_0, \dots, \beta_B)^T \in \mathbb{R}^{B+1}$  is the parameter vector.

Some recent works [32], [22] use nonlinear additive models that depend on the variables through one dimensional smooth functions. In [32] it was proved that cubic B-splines optimize a smoothness criterion on these 1D functions. Variable selection was obtained by a group lasso penalty. A similar model is presented in [34] where a coordinate descent soft thresholding algorithm is used for optimizing an  $L_1$  group-penalized loss function. Our work differs from these works by imposing constraints on the coefficients instead of biasing them with the  $L_1$  penalty. Moreover, our optimization is achieved by a novel gradual variable selection algorithm that works well in practice and is computationally efficient.

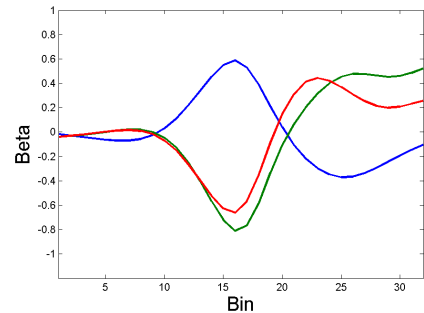


Fig. 4. Piecewise linear response functions  $f_{\beta_j}(x_j) = \mathbf{u}_j^T(x_j) \boldsymbol{\beta}_j$  obtained on an eye detection problem using the second order prior (13).

### 4.2 Nonlinear Response Regularization

Aside from the shrinkage penalty  $\rho(\boldsymbol{\beta}_j) = \lambda \|\boldsymbol{\beta}_j\|^2$ , we will experiment with the second order prior

$$\rho(\boldsymbol{\beta}_j) = \lambda \|\boldsymbol{\beta}_j\|^2 + c \sum_{k=2}^{B-1} (\beta_{j,k+1} + \beta_{j,k-1} - 2\beta_{j,k})^2 \quad (13)$$

that favors "smooth" feature response functions  $h_j(x_j)$ , as shown in Figure 4.

Other priors could be used, such as differentiable versions of the total variation regularization

$$\rho(\beta_j) = q \sum_{k=1}^B h(\beta_{j,k} - \beta_{j,k-1}) \quad (14)$$

where  $h : \mathbb{R} \rightarrow \mathbb{R}$  could be for example the Huber approximation of the  $L_1$  norm.

### 4.3 Example: Nonlinear FSA Classifier

We are interested in binary classification in an instance space  $\Omega \subset \mathbb{R}^M$ . To introduce nonlinearity, we will aggregate piecewise linear learners described in Section 4.1. Other ways to introduce nonlinearity could be used (e.g. splines) and are subject to further exploration.

Using the piecewise linear learners, we obtain the following logistic regression classifier:

$$p(\mathbf{x}, \beta) = \frac{1}{1 + \exp(-\beta_0 - \sum_{j=1}^M \mathbf{u}_j^T(x_j) \beta_j)} \quad (15)$$

where the parameter vector  $\beta = (\beta_0, \beta_1, \dots, \beta_M)$  contains the intercept  $\beta_0$  and the per-variable parameter vectors  $\beta_j \in \mathbb{R}^{B+1}$ ,  $j = 1, M$ .

The logistic loss function with the piecewise linear learners is

$$L(\beta) = - \sum_{n=1}^N w_n \ln(1 + e^{-\tilde{y}_n(\beta_0 + \sum_{j=1}^M \mathbf{u}_j^T(x_{nj}) \beta_j)}) + \sum_{j=1}^M \rho(\beta_j) \quad (16)$$

**Large Scale Implementation.** The FSA algorithm can be parallelized for large scale problems by subdividing the  $N \times M$  data matrix into a grid of sub-blocks that fit into the memory of the processing units. Then the probabilities  $p_n$  are obtained from a row-wise reduction of the partial sums  $\sum \beta_{i_j n_i}$  computed by the units. The parameter updates are done similarly, via column-wise reduction. A GPU based implementation could offer further computation cost reductions.

## 5 FSA FOR RANKING

We develop an interesting generalization of FSA to deal with ranking problems. Let  $\mathbf{x}_i \in \mathbb{R}^M$  be the training instances and  $r_{ij} \in [0, 1]$  be the true rankings between observations  $\mathbf{x}_i, \mathbf{x}_j$ , with  $(i, j) \in C \subset \{1, \dots, N\} \times \{1, \dots, N\}$ . Observe that the true ranking might not be given for all pairs  $(i, j) \in \{1, \dots, N\} \times \{1, \dots, N\}$  but only for the subset  $C$ . A criterion (e.g. an error measure) can be used to compare instances  $\mathbf{x}_i$  and  $\mathbf{x}_j$  and generate the true rankings  $r_{ij} \in [0, 1]$ , which can be for example 0 is  $\mathbf{x}_i$  is "better" than  $\mathbf{x}_j$ , 0.5 if they are "equally good" and 1 if  $\mathbf{x}_i$  is "worse" than  $\mathbf{x}_j$ .

Training means finding a ranking function  $h_\beta(\mathbf{x}) : \mathbb{R}^M \rightarrow \mathbb{R}$  specified by a parameter vector  $\beta$  such that  $h_\beta(\mathbf{x}_i) - h_\beta(\mathbf{x}_j)$  agrees as much as possible with the true rankings  $r_{ij}$ .

There are different criteria that could be optimized to measure this degree of agreement, but we will use the

differentiable criterion from [8]

$$L(\beta) = \sum_{(i,j) \in C} \ln(1 + \exp(h_\beta(\mathbf{x}_i) - h_\beta(\mathbf{x}_j))) - \sum_{(i,j) \in C} r_{ij}(h_\beta(\mathbf{x}_i) - h_\beta(\mathbf{x}_j)) + \sum_{j=1}^M \rho(\beta_j) \quad (17)$$

where we added the prior term  $\sum_{j=1}^M \rho(\beta_j)$  that helps with generalization.

### 5.1 FSA-PL For Ranking

Using the notations from Section 4.1, we can use the nonlinear ranking function

$$h_\beta(\mathbf{x}) = \sum_{k=1}^M \mathbf{u}_k^T(x_k) \beta_k, \quad (18)$$

where  $\mathbf{u}_k(x_k)$  is the basis response vector and  $\beta_k \in \mathbb{R}^{B+1}$  is the coefficient vector of variable  $k$ .

The loss function (1) in this case has the partial derivatives

$$\frac{\partial L(\beta)}{\partial \beta_k} = \sum_{i,j \in C} \left( \frac{1}{1 + e^{h_\beta(\mathbf{x}_j) - h_\beta(\mathbf{x}_i)}} - r_{ij} \right) (\mathbf{u}_k(x_{ik}) - \mathbf{u}_k(x_{jk})) + \frac{\partial \rho(\beta_k)}{\partial \beta_k}$$

where  $x_{ik}$  is variable  $k$  of observation  $\mathbf{x}_i$ .

For ranking we use the shrinkage prior for each coefficient vector  $\beta_k \in \mathbb{R}^{B+1}$

$$\rho(\beta_k) = \lambda \|\beta_k\|^2, \quad (19)$$

which discourages large values of the coefficients.

The FSA-Rank method will be used in the next section to compare motion segmentations and choose the best one from a set of segmentations with different parameters.

## 6 RANKING FOR MOTION SEGMENTATION

A popular method for sparse motion segmentation is spectral clustering [29]. In this method the feature point trajectories are projected to a lower dimensional space where spectral clustering is performed according to an affinity measure.

A major difficulty in this approach is that a rigid motion lies in a low dimensional space that does not have a fixed dimension. As a result, when there are several motions present in the same video sequence, it is hard to determine the best projection dimension for spectral clustering.

Consequently, some segmentation methods [11], [29] propose to project to a number of spaces of different dimensions and find the best results according to some measure.

However, it is hard to find a versatile measure that is consistent in finding the best dimension in all scenarios. Also, segmentation algorithms always have one or more parameters that need to be tuned according to different

scenarios, for example, the noise level, the separability of the affinity measure, etc. It is also hard to expect there exists a set of parameters that work well for all problems.

Moreover, many motion segmentation algorithms have been published in recent years. Different algorithms have different weaknesses and work best on different datasets. It would be of practical importance to segment one sequence by many different algorithms and find an automatic way to select the best segmentation.

In this work, we address the problem of choosing the best segmentation from a larger set of segmentations that are generated by different algorithms or one algorithm with different parameters. We formalize it as a ranking problem and solve it using supervised learning with the FSA-Rank algorithm.

### 6.1 Segmentation by Spectral Clustering

The segmentation candidates are generated by the velocity clustering (VC) algorithm [11]. We state it briefly to make the paper self-contained. A trajectory  $t = [(x_1, y_1), \dots, (x_F, y_F)]$  is transformed into a velocity vector

$$v(t) = [x^1 - x^2, y^1 - y^2, \dots, x^{F-1} - x^F, y^{F-1} - y^F, x^F, y^F]^T \quad (20)$$

where  $F$  is the number of frames. Then the velocity vectors are projected to spaces of different dimensions in range  $[2K, 4K]$  by truncated SVD, where  $K$  is the number of motions. The range contains the possible dimensions of spaces containing  $K$  mixed rigid motions. At last, spectral clustering is applied to obtain the segmentation using the angular affinity

$$A_{ij} = \left( \frac{t'_i t'_j}{\|t_i\| \|t_j\|} \right)^{2\alpha}, \quad i, j \in \{1, \dots, P\} \quad (21)$$

where  $t_i$  and  $t_j$  are two points, and  $\alpha$  is a tuning parameter to improve intercluster separability. In this paper the value  $\alpha$  is set to 2, as in VC [11]. Please refer to [11] for more details.

After removing possible repetitive segmentations, around  $2K + 1$  segmentations would be generated for each sequence.

While the VC proposes a error measure to select the best segmentation, this paper solves the same problem by learning.

### 6.2 Likelihood and Prior Based Features

A motion segmentation can be described by a labeling  $L : \{1, \dots, P\} \rightarrow \{1, \dots, K\}$ . We will use two types of features that can characterize the ranking of a motion segmentation  $L$ : likelihood features and prior features.

Under the orthographic camera assumptions, the point trajectories of each rigid motion should lie in a 3 dimensional affine subspace.

For a segmentation the **likelihood features** are used to measure how far are the point trajectories of the same label from lying in a 3D linear subspace.

For both the original trajectory vectors and the points obtained by projection to space of dimension  $d$ , where  $d$  is a parameter, we fit in a least squares sense 3-D affine subspaces  $S_l$  through the points of motion label  $l \in \{1, \dots, K\}$ . Denote  $L(i)$  as the label of trajectory  $t_i$  and let  $D(t, S)$  be the euclidean distance of point  $t$  to plane  $S$ . Let  $N$  is the total number of trajectories.

We use three types of likelihood features:

- The average distance

$$\frac{1}{N} \sum_{i=1}^N D(t_i, S_{L(i)})$$

- The average squared distance

$$\frac{1}{N} \sum_{i=1}^N D^2(t_i, S_{L(i)})$$

- The average thresholded distance

$$\frac{1}{N} \sum_{i=1}^N I(D(t_i, S_{L(i)}) \geq \tau),$$

where  $I(\cdot)$  is the indicator function taking on value 1 if its argument is true or 0 otherwise, and  $\tau$  is a threshold.

Inspired by VC, the first and second types of features obtained in dimensions  $d \in [2K, 4K]$  are sorted and the smallest 4 are used as features.

By changing the threshold  $\tau$  and dimension  $d$  a number of features of the third type can be obtained.

The **prior features** measure the compactness of the partition over different graphs.

For a given  $k$ , the  $k$ -nearest neighbor (kNN) graph is constructed using a distance measure in a space of a given dimension  $d$ . The distance could be either the Euclidean distance or the angular distance defined in eq. 21. By changing the dimension  $d$ , number of neighbors  $k$  and distance measure a number of different graphs and features are obtained.

On the kNN graph  $G = (V, E)$  the prior feature is the proportion of the edges that connect vertices with different labels

$$F_G = \frac{|(i, j) \in E, L(i) \neq L(j)|}{|E|}$$

where  $L(i)$  is the segmentation label of vertex  $i \in V$ .

In total, the features described in this section result in more than 2000 features for each segmentation.

### 6.3 Training the Ranking Function

The performance of a segmentation is characterized by misclassification error

$$\text{Misclassification Error} = \frac{\# \text{ misclassified points}}{\text{total \# of points}}, \quad (22)$$

which could be easily calculated by comparing with the ground truth segmentation.

The true rankings  $r_{ij}, (i, j) \in C$  is constructed based on the relative misclassification errors of the segmentations. Since at test time only segmentations belonging to the

same sequence will be compared, the set  $C$  contains only pairs of segmentations obtained from the same sequence.

For any two segmentations  $i, j$  obtained from the same sequence, the ranking  $r_{ij}$  is based on the misclassification errors of the two segmentations, with value 1 if  $i$  is better than  $j$ , 0.5 if they have the same error and 0 if  $j$  is better than  $i$ .

These ground truth rankings and the feature vectors for each segmentation are used in the FSA-Rank Algorithm to obtain the parameter vector  $\beta$  that generates the ranking function  $h_\beta(x)$  from eq. (18).

## 6.4 Motion Segmentation Algorithm

Given a new sequence, the learned parameter vector  $\beta$  is used to select the best segmentation for that sequence. The whole procedure is described in Algorithm 2.

---

### Algorithm 2 Motion Segmentation using Ranking

---

**Input:** The measurement matrix  $W = [t_1, t_2, \dots, t_P] \in \mathbb{R}^{2F \times P}$  whose columns are point trajectories, and the number of clusters  $K$ .

**Preprocessing:** Build the velocity measurement matrix  $W' = (v(t_1), \dots, v(t_P))$  where  $v(t)$  is given in eq. (20).

**for**  $d = d_{min}$  **to**  $d_{max}$  **do**

1. Perform SVD:  $W' = U\Sigma V^T$

2. Obtain  $P$  projected points as the columns of the  $d \times P$  matrix

$$X_d = [v_1, \dots, v_d]^T$$

where  $v_i$  is the  $i$ -th column of  $V$ .

3. Apply spectral clustering to the  $P$  points of  $X_d$  using the affinity measure (21), obtaining segmentation  $L_d$ .

4. Extract feature vector  $x_d$  from segmentation  $L_d$  as described in Section 6.2.

5. Compute the ranking

$$h(L_d) = \sum_{k=1}^M \mathbf{u}_k^T(x_{dk})\beta_k$$

**end for**

**Output:** The segmentation result  $L_d$  with the largest value of  $h(L_d)$ .

---

## 7 EXPERIMENTS ON REAL DATA

We present FSA experiments on face keypoint detection using classification and regression and on motion segmentation using ranking.

### 7.1 Face Keypoint Detection Experiments

As this work is intended to be used in computer vision, we present experiments on detecting face keypoints from color images. The face keypoints such as eye centers, mouth corners, chin, ear canal, are represented as 2D points  $(x, y)$ .

**AFLW.** The dataset used for training and testing is the AFLW dataset [25], which has 21123 images containing 24386 faces annotated with 21 points. Of them, 16207 images were found to contain one face per image and were split into two disjoint sets, one of 999 images for training (AFLWT) and 15208 images for testing (AFLW1). There were 2164 images containing at least 2 annotated faces. By visual inspection, 1555 of them were found to have all the faces annotated and were used as the test dataset AFLWMF. These 1555 images contained 3861 faces.

**Feature pool.** All classifiers were trained using a feature pool consisting of  $288 \cdot 3 = 864$  Histograms of Oriented Gradients (HOG) features [10] and 61000 Haar features extracted from the RGB channels in a  $24 \times 24$  pixel window centered at the point of interest  $(x, y)$  in one of the images of a Gaussian pyramid with 4 scales per octave (i.e. resized by powers of  $2^{1/4}$ ).

**Training examples.** The training examples are points on the Gaussian pyramid, with the positives within one pixel from the keypoint annotation on the images of the pyramid where the inter-eye distance is in the  $[20, 40]$  pixel range. The negatives are all points at least 4 pixels from the keypoint annotation. In total the 999 AFLW training images contain about 1 billion negatives. All the negatives were used for training the classifiers through a negative mining procedure similar to [17], with the difference that the hard negatives were added to the training set, thus the set of training negatives increased with each mining iteration. A separate classifier was trained for each keypoint, with 10 iterations of mining hard negatives.

**Algorithms.** We compared the following learning algorithms:

- 1) FSA-SVM - The FSA method on the SVM loss (7) with piecewise linear learners,  $v = 200, N^{iter} = 500$ .
- 2) LB - Logitboost using univariate piecewise constant regressors as weak learners. Only 10% of the learners were selected at random and trained at each boosting iteration and the best one was added to the classifier.
- 3) SVM-PL HOG - The SVM algorithm with piecewise linear response on each variable. The variables were the 864 HOG features.

**Classifier size** A separate classifier was trained for each keypoint being evaluated. The FSA-SVM and LB classifiers were trained as monolithic classifier with 1500 features or weak learners. The SVM-PL HOG classifier was trained on its 864 features.

**Detection criteria.** The following criteria were used for evaluating detection performance. The visible face part is considered detected in an image if a detection is found at most 3 pixels away in one of the images of the pyramid. A detected point  $p$  in one of the images of the pyramid is a false positive if it is at least 5 pixels away from the face part being evaluated (visible or not).

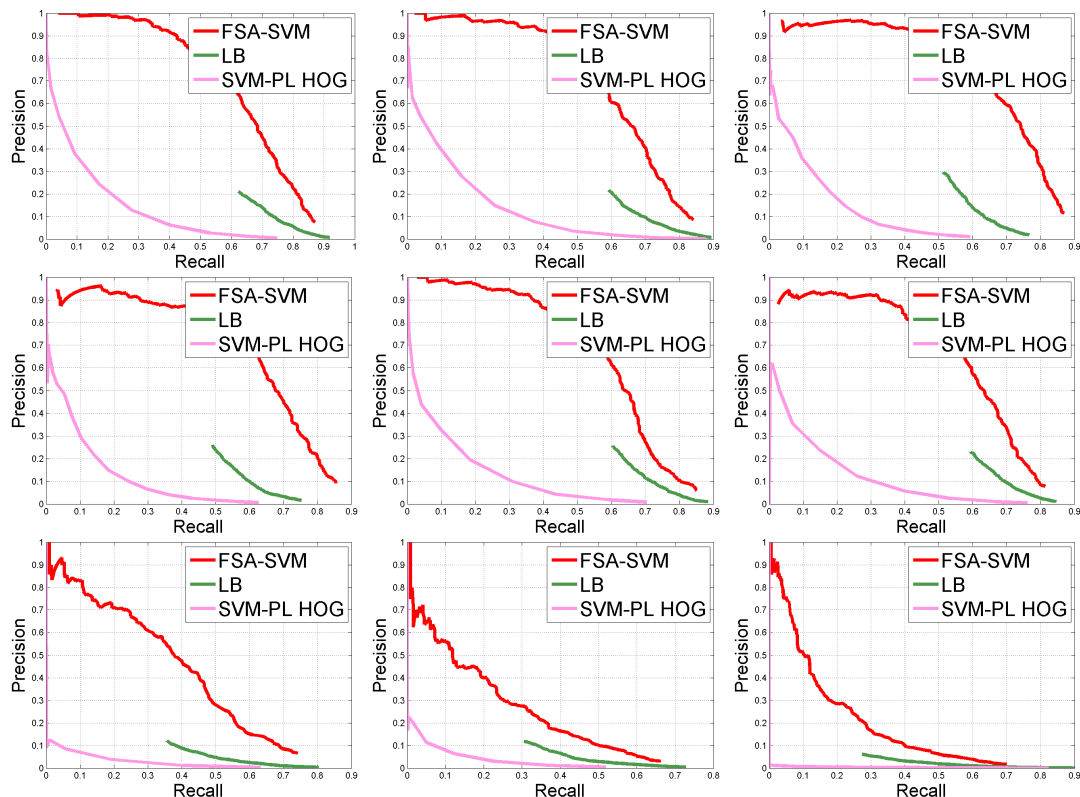


Fig. 5. Precision-recall curves for face part detection. From top to bottom, left to right: left/right eye center, left/right nose, left/right mouth corner, left/right ear, chin.



Fig. 6. Regression based object detection. Left: a regressor predicts the relative location of the object (mouth corner) from points on a sparse grid. Middle: The predicted locations are verified using a classifier. Right: The detection result.

**Results.** In Figure 5 are shown the precision-recall curves for detecting nine keypoints on the AFLWMF data. One can see that the FSA algorithm overall performs better than TISP and all the Logitboost versions. At the same time, the FSA algorithm is about 8 times faster than the LB algorithm, which is 10 times faster than the full LB version that trains all weak learners at each boosting iteration.

## 7.2 Regression Experiments

We apply the FSA regression framework to speed up the keypoint detection presented in the previous section.

### 7.2.1 Regression Based Object Detection

Applying the sliding window classifier to all locations in the image pyramid can be computationally expensive. A faster alternative is based on the fact that many times the object of interest is part of a larger context, for example the face keypoint is part of the face. The context can be used to predict the object location. This idea has been used in [42] for detecting and segmenting the left ventricle of the heart in ultrasound images.

In this paper we apply the same idea, with the difference that we used a regular grid instead of a random set of points and we applied another classifier to prune the grid locations before applying the regressor.

The keypoint detection algorithm proceeds as de-

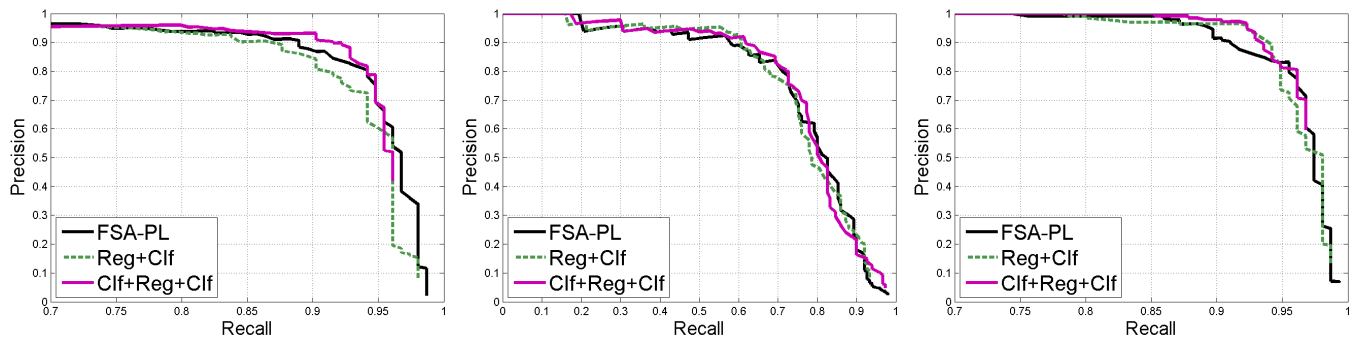


Fig. 7. Precision-recall curves for face part detection. Left: left mouth corner. Center: chin. Right: right eye pupil.

scribed in Algorithm 3. The algorithm uses the image based regressor  $f(I, x, y)$  and the classifiers  $c_0(I, x, y)$  (optional) and  $c_1(I, x, y)$ . The algorithm without the optional pruning step is also illustrated in Figure 6.

### Algorithm 3 Regression Based Keypoint Detection

**Input:** Image  $I$ .  
Set  $D = \emptyset$   
**for**  $I_s$  on a Gaussian pyramid of  $I$  **do**  
  Construct a grid  $G_s$  of equally spaced points in  $I_s$   
  (Optional) Prune the points  $G_s$  using classifier  $c_0$   
  **for**  $(x, y) \in G_s$  **do**  
    Predict  $(dx, dy) = f(I_s, x, y)$  using regressor  $f$   
    Obtain  $(x_1, y_1) = (x + dx, y + dy)$   
    **if**  $c_1(I_s, x_1, y_1) > \tau$  **then**  
      Set  $D = D \cup \{(x_1, y_1, s)\}$   
    **end if**  
  **end for**  
**end for**  
**Output:** Set of detected points  $D$ .

### 7.2.2 Regression Results

The following algorithms will be evaluated:

- 1) FSA-PL. The sliding window detector FSA-PL from Section 7.1, which applies the classifier to all locations of the image pyramid and returns the locations above a threshold.
- 2) Reg+Clf. The regression based keypoint detection algorithm 3 with a 10 pixel grid and without the optional pruning step. The classifier  $c_1$  is the same FSA-PL classifier as above.
- 3) Clf+Reg+Clf. The regression based keypoint detection algorithm 3 with a 10 pixel grid and with the optional pruning step. The classifiers  $c_0$  and  $c_1$  are trained as described below.

**Feature pool.** The regressor and classifiers are all trained with the same 61944 HOG+Haar feature pool used in Section 7.1.

**Regressor training.** The regressor has 1000 weak learners, each being a 2D univariate function  $h(x) = (\beta_1 \mathbf{u}(x), \beta_2 \mathbf{u}(x))$ .

**Classifier training.** The classifier  $c_0$  was trained using positive examples a subset of the points at distance at most 8 pixels from the true keypoint location and with negatives at distance at least 40 from the keypoint

location. It is a two node cascade of FSA-PL classifiers with 100 and 1000 features respectively.

For the Clf+Reg+Clf algorithm, the classifier  $c_1$  was trained with the same positives as the FSA-PL from section 7.1. The negatives were all locations at distance at least 4 from the true keypoint location that were not rejected by  $c_0$ . Depending on keypoint, there were between 6 million and 25 million negatives.

TABLE 4

Average detection times per image and average precision [14] on the test (unseen) data of the LFPW dataset.

Method	Avg. Detection Time per image (sec)	Average Precision		
		L Mouth	Chin	R Eye
FSA-PL	1.79	0.886	0.746	0.901
Reg+Clf	0.95	0.877	0.748	0.905
Clf+Reg+Clf	0.48	0.891	0.749	0.907

**Results.** The results are summarized in Table 4 and the precision-recall curves are shown in Figure 7.

One could see that the Reg+Clf algorithm performs similarly with the sliding window classifier and the Clf+Reg+Clf algorithm outperforms the sliding window classifier while being three times faster. We also observed that the Clf+Reg+Clf algorithm generalizes better to unseen data than the pure classification based approach.

### 7.3 Ranking Experiments

The FSA Rank based method for motion segmentation was evaluated on the Hopkins 155 dataset [38]. The Hopkins 155 Dataset has been created with the goal of providing an extensive benchmark for testing feature based motion segmentation algorithms. It contains 155 sets of trajectories of 2 or 3 motions from 50 videos, along with the corresponding ground truth. Based on the content of the video and the type of motion, the 155 sequences can be categorized into three main groups: *checkerboard*, *traffic* and *articulated*. Figure 8 shows sample frames from three videos of the Hopkins 155 database with the feature points superimposed.

#### 7.3.1 RankBoost

The RankBoost algorithm [18] is used in this paper as a baseline method to compare performance in learning the ranking function.

Let  $S = \{\mathbf{x}_i \in \mathbb{R}^M, i = \overline{1, N}\}$  be the set of training instances. We assume that a ground truth ranking is given



Fig. 8. Sample images from some sequences of three categories in the Hopkins 155 database with ground truth superimposed.

on a subset  $C \subset \{1, \dots, N\} \times \{1, \dots, N\}$  as  $r_{ij}, (i, j) \in C$  where  $r_{ij} > 0$  means  $x_i$  should be ranked above  $x_j$  and vice versa.

RankBoost searches for a ranking which is similar to the given ranking  $r$ . To formalize the goal, a distribution  $D$  is constructed by  $D_{ij} = c \cdot \max\{0, r_{ij}\}$ , where  $c$  is a constant to make  $\sum_{(i,j) \in C} D_{ij} = 1$ . The learning algorithm tries to find a ranking function  $H : \mathbb{R}^M \rightarrow \mathbb{R}$  that minimizes the weighted sum of wrong orderings:

$$\text{rloss}_D = \sum_{(i,j) \in C} D_{ij} I(H(x_i) \leq H(x_j))$$

where again  $I(\pi)$  is 1 if predicate  $\pi$  holds and 0 otherwise. The ranking function  $H(x)$  is a weighted sum of weak rankers which are selected iteratively

$$H(x) = \sum_{t=1}^T \alpha_t h_t(x).$$

At iteration  $t$ , RankBoost selects the best weak ranker  $h_t$  along with its weighted ranking score  $\alpha_t$  from the pool of candidate weak rankers, and adds  $\alpha_t h_t(x)$  to the ranking function  $f_{t-1}(x)$ .

We used threshold-based weak rankers

$$h(x) = \begin{cases} 1 & \text{if } x_i > \theta \\ 0 & \text{if } x_i \leq \theta \end{cases} \quad (23)$$

that depend on the threshold  $\theta \in \mathbb{R}$  and the variable index  $i$ . The pool of weak rankers is generated using all variables  $i = \overline{1, M}$  and  $B = 64$  equally spaced thresholds on the range of each feature.

### 7.3.2 Misclassification Error

**Parameter Settings.** The parameters for RankBoost were the following: the number of thresholds  $B = 64$ , and the number of boosting iterations was set to 100.

The parameters for our FSA-Rank method were: number of bins  $B = 4$ , the number of features  $s = 40$ . The other parameters are  $N^{iter} = 300, \eta = 0.5, \mu = 1, \lambda = 0.01$ .

**Ten Fold Cross Validation.** The Hopkins 155 dataset contains sequences from 50 videos. The 50 videos were divided at random into 10 subsets, each subset containing 5 videos. For each subset of 5 videos were collected all the Hopkins 155 sequences corresponding to these 5 videos. This way the 155 Hopkins sequences were also divided into 10 subsets. The reason for separating the videos first and then the sequences is fairness. Some 2 motion sequences are subsets of 3 motion sequences, and

it is possible that the segmentation from 2 motions is a subset of that of 3 motions. If this happens, then it would be unfair to have a 3-motion sequence in the training set and a 2-motion subset from the same sequence for testing.

At round  $k$  of the cross validation, we select the  $k$ -th of the 10 subsets of sequences as the test set and form the training set from the remaining 9 subsets. After training, we apply the obtained ranking function to rank the motion segmentations for each sequence. The best one is picked as the final result to calculate classification rate.

**Ranking Accuracy.** Each sequence would be selected in the training set 9 times and in the test set once. In Table 5 are shown the average misclassification errors over all sequences when they were in the training set and when they were in the test set. Our method outperforms the RankBoost algorithm in every category on both training and test sets, even though Rankboost uses 100 boosting iterations (thus about 100 features) while FSA-Rank uses only 40 features.

Also the difference in misclassification rate between the training set and test set is very small for FSA-Rank, especially for 2-motion sequences. In comparison, the average misclassification rate of 3 motions on test set of RankBoost is about 50% larger than that on training set, while these two misclassification rates are quite close on our method. This is probably due to the small number of features selected and the shrinkage prior (13), which together helped obtain a small training error and good generalization.

Compared to VC [11] which uses a fixed measure to select best segmentation, our method works better on the 2 motion sequences which constitutes most of the dataset. For the 3 motion sequences, our method works better on Checkerboard and Articulated categories and worse on the Traffic category. Moreover, the average misclassification rates of our method on both 2 motions and 3 motions are almost half of those from SSC [29].

From the cumulative distributions shown in Figure 9, we see that for 2 motions our method performs much better than the other methods compared, while for 3 motions our method is comparable to the best (VC). Nevertheless, our method outperforms RankBoost in both situations.

TABLE 5  
Misclassification rate (in percent) for sequences of full trajectories in the Hopkins 155 dataset.

Method	SC	SSC	VC	RankBoost		FSARank							
						Likelihood		Features		Prior		All Features	
						Train	Test	Train	Test	Train	Test	Train	Test
Checkerboard (2 motion)													
Average	0.85	1.12	0.67	0.67	0.74	0.58	0.69	1.09	1.28	0.12	0.12		
Median	0.00	0.00	0.00	0.00	0.00	0.00	0.00	0.00	0.00	0.00	0.00		
Traffic (2 motion)													
Average	0.90	0.02	0.99	0.69	0.72	0.80	0.76	4.25	4.25	0.59	0.58		
Median	0.00	0.00	0.22	0.00	0.00	0.15	0.00	0.00	0.00	0.00	0.00		
Articulated (2 motion)													
Average	1.71	0.62	2.94	2.05	2.26	2.30	2.27	1.32	1.32	1.32	1.32		
Median	0.00	0.00	0.88	0.00	0.00	0.00	0.00	0.00	0.00	0.00	0.00		
All (2 motion)													
Average	0.94	0.82	0.96	0.80	0.87	0.80	0.85	1.93	2.05	0.35	0.35		
Median	0.00	0.00	0.00	0.00	0.00	0.00	0.00	0.00	0.00	0.00	0.00		
Checkerboard (3 motion)													
Average	2.15	2.97	0.74	0.85	2.60	0.74	0.74	4.10	4.22	0.49	0.49		
Median	0.47	0.27	0.21	0.26	0.26	0.21	0.21	0.24	0.24	0.21	0.21		
Traffic (3 motion)													
Average	1.35	0.58	1.13	4.15	4.24	1.13	1.13	4.05	4.05	1.73	1.07		
Median	0.19	0.00	0.21	0.00	0.47	0.00	0.00	0.00	0.00	0.00	0.00		
Articulated (3 motion)													
Average	4.26	1.42	5.65	3.66	18.09	5.32	5.32	3.19	3.19	3.19	3.19		
Median	4.26	0.00	5.65	3.66	18.09	5.32	5.32	3.19	3.19	3.19	3.19		
All (3 motion)													
Average	2.11	2.45	1.10	1.67	3.82	1.08	1.08	4.04	4.13	0.90	0.76		
Median	0.37	0.20	0.22	0.20	0.32	0.20	0.20	0.20	0.20	0.00	0.00		
All sequences combined													
Average	1.20	1.24	0.99	1.00	1.54	0.86	0.90	2.40	2.52	0.47	0.44		
Median	0.00	0.00	0.00	0.00	0.00	0.00	0.00	0.00	0.00	0.00	0.00		

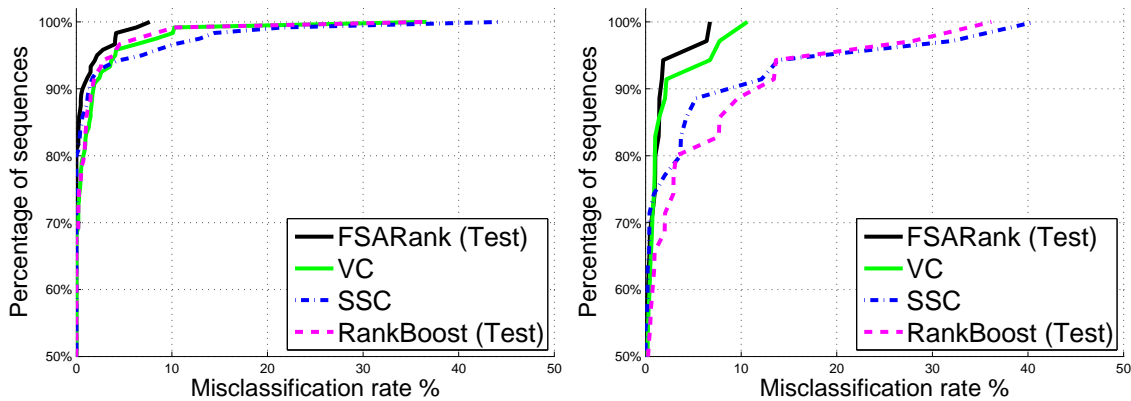


Fig. 9. The cumulative distribution of the misclassification rate for two and three motions in the Hopkins 155 database.

## 8 CONCLUSION AND FUTURE WORK

This paper presented a competitive alternative to Boosting for variable selection and classification, by optimizing a constrained penalized likelihood with a novel optimization algorithm. The proposed algorithm gradually removes variables based on a schedule specifying how many variables are left at each step, alternating variable removal with parameter updates.

Due to the simplicity of the algorithm, differentiable priors on the parameters can easily be added to the loss function, such as the second order priors used in this paper for nonlinear classification. As opposed to the  $L_1$ -penalized methods, the proposed method does not introduce any undesired biases on the parameters, property reflected in an improved prediction performance.

Due to the variable selection schedule, the total

amount of data required for training is equivalent to about 2-5 passes through the entire training set, which makes it amenable for large scale problems without being an online algorithm.

Experiments on synthetic data indicate that the proposed method finds the true variables with high probability when the number of observations is sufficiently large. The experiments demonstrate that the proposed method outperforms  $L_1$  penalized logistic regression and Logitboost (especially when selecting a large number of variables) in terms of both variable selection and prediction performance on unseen data.

In the future we plan to apply the variable selection method to challenging object detection problems.

## REFERENCES

- [1] A. Agresti. *Categorical Data Analysis*. Wiley, 2012.
- [2] A. Albert and J. A. Anderson. On the existence of maximum likelihood estimates in logistic regression models. *Biometrika*, 71(1):pp. 1–10, 1984.
- [3] A. Blake and A. Zisserman. Visual reconstruction. 1987.
- [4] P. Breheny and J. Huang. Coordinate descent algorithms for nonconvex penalized regression, with applications to biological feature selection. *The Annals of Applied Statistics*, 5(1):232–253, 2011.
- [5] A. Bruce and H. Gao. Understanding waveshrink: variance and bias estimation. *Biometrika*, 83(4):727–745, 1996.
- [6] F. Bunea, A. Tsybakov, and M. Wegkamp. Sparsity oracle inequalities for the lasso. *Electronic Journal of Statistics*, 1:169–194, 2007.
- [7] R. Burden and J. Faires. Numerical analysis. 2001. *Brooks/Cole, USA*.
- [8] C. Burges, T. Shaked, E. Renshaw, A. Lazier, M. Deeds, N. Hamilton, and G. Hullender. Learning to rank using gradient descent. In *ICML*, pages 89–96, 2005.
- [9] O. Chapelle. Training a support vector machine in the primal. *Neural Comp.*, 19(5):1155–1178, 2007.
- [10] N. Dalal and B. Triggs. Histograms of oriented gradients for human detection. In *CVPR*, pages 886–893, 2005.
- [11] L. Ding, A. Barbu, and A. Meyer-Baese. Motion segmentation by velocity clustering with estimation of subspace dimension. In *ACCV Workshop on Detection and Tracking in Challenging Environments*, 2012.
- [12] D. Donoho, M. Elad, and V. Temlyakov. Stable recovery of sparse overcomplete representations in the presence of noise. *Information Theory, IEEE Transactions on*, 52(1):6–18, 2006.
- [13] B. Efron, T. Hastie, I. Johnstone, and R. Tibshirani. Least angle regression. *The Annals of Statistics*, 32(2):407–499, 2004.
- [14] M. Everingham, L. Van Gool, C. Williams, J. Winn, and A. Zisserman. The pascal visual object classes (voc) challenge. *International Journal of Computer Vision*, 88(2):303–338, 2010.
- [15] J. Fan, Y. Feng, and R. Song. Nonparametric independence screening in sparse ultra-high-dimensional additive models. *Journal of the American Statistical Association*, 106(494):544–557, 2011.
- [16] J. Fan and R. Li. Variable selection via nonconcave penalized likelihood and its oracle properties. *Journal of the American Statistical Association*, 96(456):1348–1360, 2001.
- [17] P. Felzenszwalb, R. Girshick, D. McAllester, and D. Ramanan. Object detection with discriminatively trained part-based models. *Pattern Analysis and Machine Intelligence, IEEE Transactions on*, 32(9):1627–1645, 2010.
- [18] Y. Freund, R. Iyer, R. E. Schapire, and Y. Singer. An efficient boosting algorithm for combining preferences. *The Journal of Machine Learning Research*, 4:933–969, 2003.
- [19] J. Friedman, T. Hastie, and R. Tibshirani. Additive logistic regression: a statistical view of boosting.(with discussion and a rejoinder by the authors). *Ann. Stat.*, 28(2):337–407, 2000.
- [20] I. Guyon, S. Gunn, M. Nikravesh, and L. A. Zadeh. *Feature extraction: foundations and applications*, volume 207. Springer, 2006.
- [21] I. Guyon, J. Weston, S. Barnhill, and V. Vapnik. Gene selection for cancer classification using support vector machines. *Machine learning*, 46(1-3):389–422, 2002.
- [22] J. Huang, J. L. Horowitz, and F. Wei. Variable selection in nonparametric additive models. *Ann. Statist.*, 38(4):2282–2313, 2010.
- [23] D. Jiang and J. Huang. Majorization minimization by coordinate descent for concave penalized generalized linear models. *Technical Report*, 2011.
- [24] K. Knight and W. Fu. Asymptotics for lasso-type estimators. *Ann. Stat.*, pages 1356–1378, 2000.
- [25] M. Koestinger, P. Wohlhart, P. M. Roth, and H. Bischof. Annotated facial landmarks in the wild: A large-scale, real-world database for facial landmark localization. In *First IEEE International Workshop on Benchmarking Facial Image Analysis Technologies*, 2011.
- [26] K. Koh, S. Kim, and S. Boyd. An interior-point method for large-scale  $l_1$ -regularized logistic regression. *Journal of Machine learning research*, 8(8):1519–1555, 2007.
- [27] L. Landweber. An iteration formula for fredholm integral equations of the first kind. *American Journal of Mathematics*, 73(3):pp. 615–624, 1951.
- [28] J. Langford, L. Li, and T. Zhang. Sparse online learning via truncated gradient. *The Journal of Machine Learning Research*, 10:777–801, 2009.
- [29] F. Lauer and C. Schnorr. Spectral clustering of linear subspaces for motion segmentation. In *ICCV*, pages 678–685. IEEE, 2009.
- [30] P. Li. Robust logitboost and adaptive base class (abc) logitboost. In *UAI*, 2010.
- [31] S. Li and Z. Zhang. Floatboost learning and statistical face detection. *Pattern Analysis and Machine Intelligence, IEEE Transactions on*, 26(9):1112–1123, 2004.
- [32] L. Meier, S. van de Geer, and P. Bühlmann. High-dimensional additive modeling. *Ann. Statist.*, 37(6B):3779–3821, 2009.
- [33] G. Rätsch, T. Onoda, and K. Müller. Regularizing adaboost. In *NIPS*, pages 564–570, 1999.
- [34] L. J. L. H. Ravikumar, P. and L. Wasserman. Spam: Sparse additive models. *Journal of the Royal Statistical Society: Series B (Statistical Methodology)*, 71:1009–1030, 2009.
- [35] R. Schapire. The strength of weak learnability. *Machine learning*, 5(2):197–227, 1990.
- [36] Y. She. Thresholding-based iterative selection procedures for model selection and shrinkage. *Electronic Journal of Statistics*, 3:384–415, 2009.
- [37] Y. She. An iterative algorithm for fitting nonconvex penalized generalized linear models with grouped predictors. *Computational Statistics and Data Analysis*, 9:2976–2990, 2012.
- [38] R. Tron and R. Vidal. A benchmark for the comparison of 3-d motion segmentation algorithms. In *CVPR*, pages 1–8. IEEE, 2007.
- [39] L. Xiao. Dual averaging methods for regularized stochastic learning and online optimization. *The Journal of Machine Learning Research*, 11:2543–2596, 2010.
- [40] C. Zhang. Nearly unbiased variable selection under minimax concave penalty. *The Annals of Statistics*, 38(2):894–942, 2010.
- [41] P. Zhao and B. Yu. On model selection consistency of lasso. *Journal of Machine Learning Research*, 7(2):2541, 2007.
- [42] S. Zhou and D. Comaniciu. Shape regression machine. In *Information Processing in Medical Imaging*, pages 13–25, 2007.

## CONVERGENCE AND CONSISTENCY PROOFS

*Proof.* Due to space limitations, we mainly show the proof for classification; the proof for regression is similar (yet simpler). To characterize the iteration, we define the **quantile thresholding**  $\Theta^\#(\cdot; k, \lambda)$ , as a variant of the **hard-ridge** thresholding [36], [37]. Given  $1 \leq k \leq M$  and  $\lambda \geq 0$ ,  $\Theta^\#(\beta; k, \lambda) : \mathbb{R}^M \rightarrow \mathbb{R}^M$  is defined for any  $\beta \in \mathbb{R}^M$  such that the  $q$  largest components of  $\beta$  (in absolute value) are shrunk by a factor of  $(1 + \lambda)$  and the remaining components are all set to be zero. In the case of ties, a random tie breaking rule is used. We write  $\Theta^\#(\beta; k)$  for  $\Theta^\#(\beta; k, 0)$ . Steps 3-5 in Algorithm 1 can be characterized by

$$\beta^{(e+1)} = \Theta^\#(\beta^{(e)} + \eta \mathbf{X}^T (y - \left[ \frac{1}{1 + e^{-\mathbf{X}\beta^{(e)}}} \right]); M_e) \quad (24)$$

$$d = \{j : \beta_j^{(e+1)} \neq 0\} \quad (25)$$

$$\beta^{(e+1)} = \beta^{(e+1)}[d] \quad (26)$$

$$\mathbf{X} = \mathbf{X}[:, d] \quad (27)$$

where  $\left[ \frac{1}{1 + e^{-\mathbf{X}\beta^{(e)}}} \right]$  is an  $N \times 1$  vector with all operations componentwise except for the matrix-vector multiplication  $\mathbf{X}\beta^{(e)}$ . For notational simplicity, introduce  $\mu(t) = 1/(1 + \exp(-t))$  and  $\mu(\xi)$  is defined componentwise for any  $\xi \in \mathbb{R}^n$ . The Fisher information matrix at  $\beta$  is denoted by  $\mathcal{I}(\mathbf{X}, \beta) = \mathbf{X}^T \text{diag} \{ \mu(\mathbf{x}_i^T \beta) (1 - \mu(\mathbf{x}_i^T \beta)) \}_{i=1}^N \mathbf{X}$ .

**Part (i):** We show that the following property holds for any  $e$  large enough:

$$F(\beta^{(e)}) \geq F(\beta^{(e+1)}), \text{ and } \|\beta^{(e)}\|_0 \leq k. \quad (28)$$

This indicates that the design of the algorithm is for the purpose of solving  $\min_{\beta} F(\beta)$  s.t.  $\|\beta\|_0 \leq k$ .

We begin by analyzing the sequence of iterates defined by

$$\beta^{(e+1)} = \Theta^\# \left( \beta^{(e)} + \eta^{(e)} \mathbf{X}^T \left( y - \mu(\mathbf{X}\beta^{(e)}) \right); k \right) \quad (29)$$

where  $\eta^{(e)}$  stand for the step sizes. Here,  $M_e = k \leq M$ , but  $M$  is possibly larger than  $N$ . Recall that  $F(\beta) = \sum_i (-y_i \mathbf{x}_i^T \beta + \log(1 + \exp(\mathbf{x}_i^T \beta)))$  for classification.

**Lemma 8.1:** Suppose  $0 < \eta^{(e)} \leq 4/\|\mathbf{X}\|_2^2$ , then for the iterates defined by (29), we have  $F(\beta^{(e)}) - F(\beta^{(e+1)}) \geq \frac{\eta^{(e)} - \|\mathbf{X}\|_2^2/4}{2} \|\beta^{(e+1)} - \beta^{(e)}\|_2^2$  and  $\beta^{(e)}$  obeys  $\|\beta^{(e)}\|_0 \leq k$ .

*Proof.* Define a surrogate function

$$G(\beta, \gamma; \omega) = \sum_i \{-y_i \mathbf{x}_i^T \gamma + \log(1 + e^{\mathbf{x}_i^T \gamma})\} + \frac{\omega}{2} \|\gamma - \beta\|_2^2 - \sum_i \{\log(1 + e^{\mathbf{x}_i^T \gamma}) + \log(1 + e^{\mathbf{x}_i^T \beta})\} + \sum_i \frac{\mathbf{x}_i^T \gamma - \mathbf{x}_i^T \beta}{1 + e^{-\mathbf{x}_i^T \beta}}.$$

Given  $\beta$ , minimizing  $G$  over  $\{\gamma : \|\gamma\|_0 \leq k\}$  is equivalent to  $\min_{\gamma} \frac{\omega}{2} \left\| \gamma - \beta - \frac{1}{\omega} \mathbf{X}^T y + \frac{1}{\omega} \mathbf{X}^T \left[ \frac{1}{1 + e^{-\mathbf{X}\beta}} \right] \right\|_2^2$  s.t.  $\|\gamma\|_0 \leq k$ .

It is easy to verify that for such a problem (though nonconvex) a globally optimal solution is given by the

quantile thresholding [37]

$$\gamma = \Theta^\# \left( \beta + \frac{1}{\omega} \mathbf{X}^T (y - \mu(\mathbf{X}\beta)); k \right).$$

On the other hand, Taylor expansion gives

$$\begin{aligned} & \sum_i \{\log(1 + e^{\mathbf{x}_i^T \gamma}) - \log(1 + e^{\mathbf{x}_i^T \beta})\} - \sum_i \frac{\mathbf{x}_i^T \gamma - \mathbf{x}_i^T \beta}{1 + e^{-\mathbf{x}_i^T \beta}} \\ &= \frac{1}{2} (\gamma - \beta)^T \mathcal{I} (\gamma - \beta), \end{aligned}$$

where  $\mathcal{I} = \mathbf{X}^T \text{diag} \left\{ \frac{e^{\mathbf{x}_i^T \zeta}}{(1 + e^{\mathbf{x}_i^T \zeta})^2} \right\}_{i=1}^N \mathbf{X}$  with  $\zeta = t\beta + (1 - t)\gamma$  for some  $t \in [0, 1]$ . It follows that  $\frac{1}{2} (\gamma - \beta)^T \mathcal{I} (\gamma - \beta) \in \left[ 0, \frac{1}{2} \frac{\|\mathbf{X}\|_2^2}{4} \|\gamma - \beta\|_2^2 \right]$

Therefore, for the sequence of  $\beta^{(e)}$  defined by (29), we have  $F(\beta^{(e+1)}) + \frac{\eta^{(e)}}{2} \|\beta^{(e+1)} - \beta^{(e)}\|_2^2 - \frac{1}{2} \frac{\|\mathbf{X}\|_2^2}{4} \|\beta^{(e+1)} - \beta^{(e)}\|_2^2 \leq G(\beta^{(e)}, \beta^{(e+1)}; \eta^{(e)}) \leq G(\beta^{(e)}, \beta^{(e)}; \eta^{(e)}) = F(\beta^{(e)})$ . That is,  $F(\beta^{(e)}) - F(\beta^{(e+1)}) \geq \frac{\eta^{(e)} - \|\mathbf{X}\|_2^2/4}{2} \|\beta^{(e+1)} - \beta^{(e)}\|_2^2$ .  $\square$

For the iterates yielded by the original algorithm, notice that  $M_e$  used in Step (24) equals  $k$  eventually, say, for any  $e > E$ , and thus  $d$  and  $\mathbf{X}$  stay fixed afterwards. From the lemma,  $F(\beta^{(e)})$  must be decreasing for  $e > E$ .

*Remark:* The result implies that in implementation, we may adopt a universal choice of the stepsize  $\eta$  at any iteration, as long as it satisfies  $\eta \leq 4/\|\mathbf{X}\|_2^2$ .

**Part (ii):** Now we prove the strict convergence of  $\beta^{(e)}$  (which is much stronger than that of  $F(\beta^{(e)})$ ). Without loss of generality, suppose  $M_e = k = M$  in (29) and thus (25)-(27) are inactive. Unlike Gaussian regression, the plain logistic regression may not have a finite ML solution, say, when the class labels having  $y = 0$  and having  $y = 1$  do not overlap in the predictor space [2]. One way to avoid such irregularities is to make an overlap assumption (which is however not needed either in regression as pointed out at the end of the proof, or when there is an additional  $\ell_2$  penalty  $\lambda \|\beta\|_2^2$  with  $\lambda > 0$ ).

**Overlap Condition.** For any  $k$ -subset of the  $M$  given  $x$ -features, neither *complete separation* nor *quasicomplete separation* [1] occurs.

Let  $\beta^*$  be a solution to

$$\mathbf{X}^T \mu(\mathbf{X}\beta) - \mathbf{X}^T y = 0, \quad (30)$$

with the existence guaranteed under the overlap assumption (see [1] for details). Let the SVD of  $\mathbf{X}$  be  $\mathbf{X} = \mathbf{U}\mathbf{D}\mathbf{V}^T$  where  $\mathbf{D}$  is a square matrix with all diagonal entries positive. Let  $\mathbf{V}_\perp$  be an orthogonal complement to  $\mathbf{V}$ . Define  $\tilde{\beta}^* = \mathbf{V}\mathbf{V}^T \beta^* + \mathbf{V}_\perp \mathbf{V}_\perp^T \beta^{(0)}$  which still satisfies (30); for simplicity, we write  $\tilde{\beta}^*$  as  $\beta^*$ . Then with a bit algebra and the Taylor expansion,  $\beta^{(e+1)} - \beta^* = (\mathbf{I} - \eta \mathcal{I}(\mathbf{X}, \zeta)) (\beta^{(e)} - \beta^*)$ . To deal with the challenge that  $\mathbf{X}^T \text{diag} \{ \mu(\mathbf{x}_i^T \zeta) (1 - \mu(\mathbf{x}_i^T \zeta)) \} \mathbf{X}$  may be singular (and thus the iteration is not a contraction), introduce  $\gamma = \mathbf{D}\mathbf{V}^T \beta; \gamma^{(e)}, \gamma^*$  are defined similarly. Then  $\gamma^{(e+1)} - \gamma^* = (\mathbf{I} - \eta \mathbf{D}^2 \mathbf{U}^T \text{diag} \{ \mu(\mathbf{x}_i^T \zeta) (1 - \mu(\mathbf{x}_i^T \zeta)) \} \mathbf{U}) (\gamma^{(e+1)} - \gamma^*)$ .

Under the  $\eta$ -assumption,  $\gamma^{(e)}$  converges (geometrically fast). By construction,  $\mathbf{V}\mathbf{V}^T(\beta^{(e)} - \beta^*) = (\beta^{(e)} - \beta^*)$  for any  $e$ , and thus  $\beta^{(e)} - \beta^* = \mathbf{V}\mathbf{D}^{-1}(\gamma^{(e)} - \gamma^*)$ . This indicates that the sequence of  $\beta^{(e)}$  strictly converges and the limit point (denoted by  $\beta_o(N)$ ) satisfies (30). Its local optimality is straightforward, because the perturbation cannot change the support of  $\beta_o(N)$  in the constrained optimization.

**Part (iii):** We construct a two-stage cooling schedule to show the consistency. Recall the assumption  $\mathcal{I}(\mathbf{X}, \beta^*)/N \rightarrow \mathcal{I}^*$ . Let  $\beta_o(N)$  be a solution to (30). From the central limit theorem,  $\sqrt{N}(\beta_o(N) - \beta^*) \Rightarrow N(0, \mathcal{I}^{*-1})$ . This indicates that with probability tending to 1,  $\beta_o(N)$  is the unique solution.

Stage 1. Set  $M_e = M$  ( $1 \leq e \leq E_0$ ) for some  $E_0$ . Accordingly, squeezing operations (25)-(27) do not take any essential effect. To bound the estimation error, we write  $\|\beta^{(e)} - \beta^*\|_\infty \leq \|\beta_o(N) - \beta^*\|_\infty + \|\beta^{(e)} - \beta_o(N)\|_\infty$ . The first term on the right hand side is at  $O_p(\frac{1}{\sqrt{N}})$  based on the central limit theorem, and thus  $o_p(1)$ . Define  $S^* = \{j : \beta_j^* \neq 0\}$  and  $\min|\beta_{S^*}^*| = \min_{j \in S^*} |\beta_j^*|$ . Then  $\|\beta_o(N) - \beta^*\|_\infty \leq \frac{1}{8} \min|\beta_{S^*}^*|$  with probability tending to 1 as  $N \rightarrow \infty$ . On the other hand, from the algorithmic convergence of  $\beta^{(e)}$  established above, there exists  $E_1$  (or  $E_1(N)$ , as a matter of fact) large enough such that  $\|\beta^{(e)} - \beta_o(N)\|_\infty \leq \frac{1}{8} \min|\beta_{S^*}^*|$  and  $\|\mathbf{X}^T \mu(\mathbf{X}\beta^{(e)}) - \mathbf{X}^T y\|_\infty \leq \frac{1}{8\eta} \min|\beta_{S^*}^*|$ ,  $\forall e \geq E_1$ . Therefore, if we choose  $E_0 \geq E_1$ ,  $\|\beta^{(e)} - \beta^*\|_\infty \leq \frac{1}{4} \min|\beta_{S^*}^*|$  and  $\|\mathbf{X}^T \mu(\mathbf{X}\beta^{(e)}) - \mathbf{X}^T y\|_\infty \leq \frac{1}{8\eta} \min|\beta_{S^*}^*|$ , for  $\forall e : E_1 \leq e \leq E_0$  occur with probability tending to 1.

Stage 2. Now set  $M_e = k \geq \|\beta^*\|_0$ ,  $\forall e > E_0$ . At  $e = E_0 + 1$ , letting  $\xi = \beta^{(e)} + \eta \mathbf{X}^T (y - \mu(\mathbf{X}\beta^{(e)}))$ , we have  $\min|\xi_{S^*}| \geq \frac{5}{8} \min|\beta_{S^*}^*| > \frac{3}{8} \min|\beta_{S^*}^*| \geq \max|\xi_{S^*c}|$ . Therefore, Step (24) yields  $\beta_j^{(e+1)} \neq 0$ ,  $\forall j \in S^*$ . After Steps (25)-(27), all relevant predictors are kept with probability tending to 1. Repeating the argument in Stage 1 gives the consistency of  $\beta^{(e)}$  for any  $e$  sufficiently large.

The proof in the Gaussian case follows the same lines. But in Part (ii) we do not have to assume the overlap condition (or require  $N \geq M$ ), due to Landweber's classical convergence result [27].